Uptake of transferrin-conjugated quantum dots in single living cells

Danni Chen (陈丹妮)[1,2], Gaixia Xu (许改霞)[2], Bahi Ahmed Ali[3,4], Ken-Tye Yong[5], Cuihong Zhou (周翠红)[3], Xiaomei Wang (王晓梅)[3], Junle Qu (屈军乐)[2], Paras N. Prasad[6], and Hanben Niu (牛憨笨)[2*]

[1] *College of Optoelectronic Science and Engineering, Huazhong University of Science and Technology, Wuhan 430074, China*

[2] *Institute of Optoelectronics, Key Lab of Optoelectronics Devices and Systems of Ministry of Education/Guangdong Province, Shenzhen Key Lab of Biomedicine Engineering, Shenzhen University, Shenzhen 518060, China*

[3] *College of Medicine, Shenzhen University, Shenzhen 518060, China*

[4] *Mubarak City for Scientific Research and Technology Applications, New Borg Al-Arab City, Alexandria 21934, Egypt*

[5] *School of Electrical and Electronic Engineering, Nanyang Technological University, Singapore 639798, Singapore*

[6] *Institute for Laser, Photonics and Biophotonics, State University of New York at Buffalo, NY 14260-3000, USA*

[*] *E-mail: hbniu@szu.edu.cn*

Received June 17, 2010

We study the uptake and distribution of transferrin (Tf)-conjugated CdSe/CdS/ZnS quantum dots (QDs) in single living HeLa cells with both fluorescence confocal microscopy and three-dimensional (3D) reconstruction technique. By increasing the co-incubation time or the dosage of QDs-Tf, we find that the uptake of QDs-Tf bioconjugates in the cells increases correspondingly, but with different uptake rates. Additionally, the distribution of QDs-Tf, in single live HeLa cells is time dependent. To our knowledge, this is the first study on quantitatively analyzing the uptake and distribution of bioconjugated QDs in single living cells. Such QDs nanoplatform can be further modified for developing biomedical evaluation tool in cancer diagnosis and targeted drug delivery.

OCIS code: 170.6280, 170.1530.
doi: 10.3788/COL2010810.0940.

Quantum dots (QDs) are emerging as a new class of luminescence probes for biology and medicine research applications[1−3]. QDs possess unique optical tunability, such as size-tunable emission wavelength, superior signal brightness, resistance to photobleaching, and broad absorption spectra for simultaneous excitation of multiple fluorescence colors using a single excitation source[4−6]. In addition, QDs provide a versatile platform for designing multifunctional nanoparticles with both imaging and therapeutic functions for disease sensing and therapy[7,8]. For example, linked with cancer specific targeting moieties such as antibodies, peptides, or other small therapeutic molecules, the bioconjugated QDs can be employed to label cancerous areas with high specific affinity[9−11]. More importantly, one can visualize the labeling dynamic process of the bioconjugated QDs in the cellular level using appropriate imaging setup such as confocal microscopy and multi-photon imaging techniques[12,13].

To date, several strategies have been used for targeting cancer cells *in vitro* by using functionalized QDs. One of them is receptor mediated approach by linking cancer specific biomolecules on the QDs surface for targeted delivery[14]. For example, some studies demonstrated that transferrin (Tf)-conjugated QDs can be used as probes for cancer cells labeling[10]. Tf is a kind of circulatory iron carrier protein for the uptake of iron in metabolically active cells[15]. Iron is highly demanded by tumor cells and transferrin receptors (TfRs) upregulated on many human tumor types. It has been revealed that tumor cells overexpress TfRs, i.e., more than 10^5 receptors per cell in several cancer cell lines, such as HeLa, HT-29 (human colon carcinoma cells), K562 (human erythroleukemia cells), and pancreatic tumor cells, compared with very low levels of TfR in normal cells[16]. Thus, Tf has emerged as a carrier for specific delivery of QDs to tumor cells.

In this letter, QDs-Tf is used as specific probes to study the distribution and localization of the bioconjugated QDs in living cancer cells by using fluorescence confocal microscopy and three-dimensional (3D) reconstruction technique. And then, the dependence of the uptake of QDs-Tf in single living HeLa cells on co-incubation time and dosage of QDs-Tf is quantitatively evaluated. The potential application of such bioconjugated QDs as novel optical targeted drug carriers is also discussed.

CdSe/CdS/ZnS QDs were prepared by growing CdS/ZnS-graded shell on CdSe core. Briefly, the reaction was carried out by mixing CdSe core QDs with Cd, Zn, and S precursors and oleic acid at 300 °C. The weight of CdSe core QDs used here was 0.3 g and the Cd:Zn:S ratio used for shell coating was 1:3:4. The CdS initially preferred to grow on the CdSe dots because the CdSe lattice mismatch with CdS is less than that of ZnS. The CdS layer mediated the growth of the more strained ZnS. The shell was uniformly and epitaxially grown and eventually coated on the CdSe core. The QDs were separated from the surfactant solution by the addition of ethanol and centrifugation. The reddish QD precipitate was readily redispersed in various organic solvents (hexane, toluene, and chloroform).

Typically, 3-mmol mercaptoundecanoic acid (MUA)

was dissolved in 10 ml of chloroform under vigorous stirring. After stirring for 10−15 min, 2 ml of concentrated (∼30 mg/ml) CdSe/CdS/ZnS QD solution was added into this mixture. Approximately one minute later, 2 ml of ammonium hydroxide was added to the vigorously stirring solution, and then was stirred overnight at room temperature. The QDs were separated from the surfactant solution by addition of ethanol and centrifugation. The QD precipitate was re-dissolved in 15 ml of dimethyl sulfoxide (DMSO) for further lysine cross-linking process. The lysine cross-linked MUA QDs were obtained by mixing DMSO QDs solution with both 1,3-dicyclohexylcarbodiimide (DCC) (∼30 mmol) and lysine (∼15 mmol) under vigorous stirring for 2 h. The lysine coated QDs were precipitated from the solution by addition of ethanol and centrifugation. The red-brownish precipitate was redispersed in 10-ml high performance liquid chromatography (HPLC) water and the solution was further filtered using a syringe filter with a nominal pore diameter of 0.45 μm. The lysine coated QDs had relatively good colloidal stability and no precipitation was observed after several months. This stock solution was kept in the refrigerator at 4 °C for further use.

Briefly, 50 ml of 46-nmol/L lysine-coated QDs stock solution was mixed with 2 ml of 2.5-nmol/L N-(3-dimethylaminopropyl)-N-ethylcarbodiimide hydrochloride (EDC) solution and the solution was gently stirred for 2−3 min. About 100 ml of 2-mg/ml Tf was added into this mixture and gently stirred at room temperature for 2 h to allow the protein to covalently bind with the lysine-coated QDs. The QDs-Tf bioconjugates were further purified by centrifugation, and filtered by syringe with a pore diameter of 0.45 μm.

In order to study the cellular uptake of the QDs-Tf bioconjugates, HeLa cells (ATCC, Manassas, VA) were cultured in Eagle's minimum essential medium supplemented with 10% fetal bovine serum in a humid incubator (37 °C and 5% CO_2). Cells were seeded in 35-mm culture dishes at a confluency of 70%. The cells in serum-supplemented media were co-incubated with the Tf-conjugated QDs at a final concentration of 100 nmol/L. After treatment, the cells were washed thrice with phosphate buffered saline (PBS) and then imaged directly using a confocal microscope. In dose-dependence experiments, different doses of QDs-Tf bioconjugates and unconjugated QDs (1, 2.5, 5.0, 10.0, and 20.0 pmol) were added into the culture medium. After 2 h of incubation, the cell culture dishes were washed thrice with fresh culture medium before performing the imaging experiments. In time dependence experiments, several time-points were selected to study the uptake and distribution of QDs-Tf bioconjugates in the HeLa cells. The dose of QDs-Tf bioconjugates added into each dish was 5 pmol. After incubation for 1, 2, 6, and 22 h, the labeled cells were individually examined at each time point.

All images were obtained by a laser scanning confocal microscope (TCS SP2, Leica). The excitation wavelength used in this study is 488 nm. Since the common dyes are susceptible to photobleaching and are not suitable for Z-stack scanning, we recorded reflection signals as background contrast. Both reflection and fluorescence images were obtained for cancer cells labeled with bioconjugated QDs, and acquired simultaneously using the two-wavelength band-selected channels. The wavelength band setups for collecting reflection and fluorescence images were 480−500 and 580−620 nm, respectively. The experimental conditions were optimized and kept consistent, including the laser power, the gain of the detector, photomultiplier tubes, and the exposure time.

In order to obtain the precise location of QDs-Tf bioconjugates and quantitatively analyze the uptake of QDs-Tf bioconjugates in living HeLa cells, Z-stack reflection and fluorescence images of single cells were acquired by means of optical sectioning imaging. The step length in Z-stack was selected according to the Nyquist sampling theorem, which ensures that no fluorescence signal from QDs would be ignored or repeated counting. These raw reflection and fluorescence images were processed with ImageJ. In brief, all the reflection and fluorescence images from the same z-positions were overlapped together to render the reconstructed images. The gray level of each pixel of the reconstructed fluorescence image was summed, as a quantificational parameter in describing the quantity of uptake. In dose-dependence experiments, the characteristics of the uptake of the targeted QDs bioconjugates under different concentrations were studied. While in time-dependence experiments, several time points were selected to investigate the uptake process of QDs-Tf bioconjugates by HeLa cells. In order to minimize the effect of cell heterogeneity on QDs-Tf bioconjugates uptaking, data from 3−4 normal single HeLa cells were averaged.

Figure 1(a) shows a transmission electron microscope (TEM) image of lysine-coated CdSe/CdS/ZnS QDs dispersed in water. According to the absorption and photoluminescence (PL) spectra shown in Fig. 1(b), the monodispersed QDs have an emission peak at 603 nm. These lysine-coated QDs can be directly used for cell staining without any sign of quenching effects. The PL

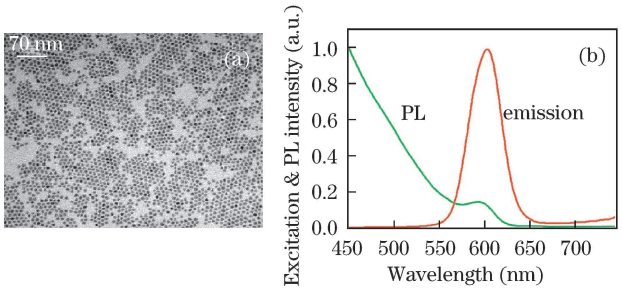

Fig. 1. (a) TEM image and (b) spectra from the largely monodispersed lysine-coated CdSe/CdS/ZnS QDs.

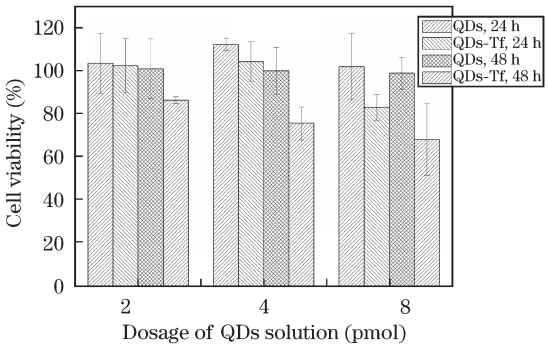

Fig. 2. MTS assay for viability of cells stained by QD or QDs-Tf bioconjugates for 24 and 48 h.

quantum yield is estimated to be 50%.

Prior to treating the HeLa cells with QDs-Tf bioconjugates, the cyctotoxicity effect of lysine-coated QDs and QDs-Tf bioconjugates on the HeLa cells was systematically investigated. Figure 2 shows the *in vitro* cytotoxicity effects of lysine-coated QDs and bioconjugated QDs on the HeLa cells by colorimetric cell viability (MTS) assay. At low dosage of treatment (∼2-pmol QDs or QDs-Tf), the cell viability treated by QDs-Tf for 48 h was 84%. However, when 8.0-pmol bioconjugated QDs were added into the HeLa cells, the cell viability dramatically reduced to 69%. It indicates that such lysine-coated QDs still have cytotoxicity for cells. However, we can use them as efficient nanoprobes at an acceptale dosage. In addition, an interesting phenomenon was that the targeted QDs had lower cell viability than non-targeted QDs. Considering that the unocupied TfRs will ferry iron-loaded Tf into cell, we think that the QDs-Tf has been transported into cells in receptor-mediated pathway, which induces the lower cell viability of targeted QDs.

Figure 3 shows the confocal microscopy images of HeLa cells stained with bioconjugated QDs for 2 h. The reflection image shows the morphology of HeLa cells. Nucleus of the cells can be distinguished clearly, which is shown as hollow areas inside cells (Fig. 3(a)). The fluorescence image indicates the distribution of QDs-Tf bioconjugates on the cells (Fig. 3(b)). The overlay image of reflection and fluorescence (Fig. 3(c)) indicates that most bioconjugated QDs are located on the cells membrane, and no bioconjugated QDs are found inside nucleus. Local spectral analysis confirms that the florescence signal is indeed from QDs (Fig. 3(d)).

However, it should be noted that cells consist of complex 3D skeleton and sub-cellular components. The two-dimensional (2D) analysis of fluorescence with confocal microscopy cannot provide the exact locations of the QD bioconjugates in cells. Present study demonstrates that 3D reconstruction technique is useful to analyze the targets of the potential novel pharmaceuticals in the living cancer cells quantitatively. Z-stack fluorescence images of labeled cells were obtained by the confocal microscopy. Subsequently, ImageJ software was employed to reconstruct the 3D image based on these images.

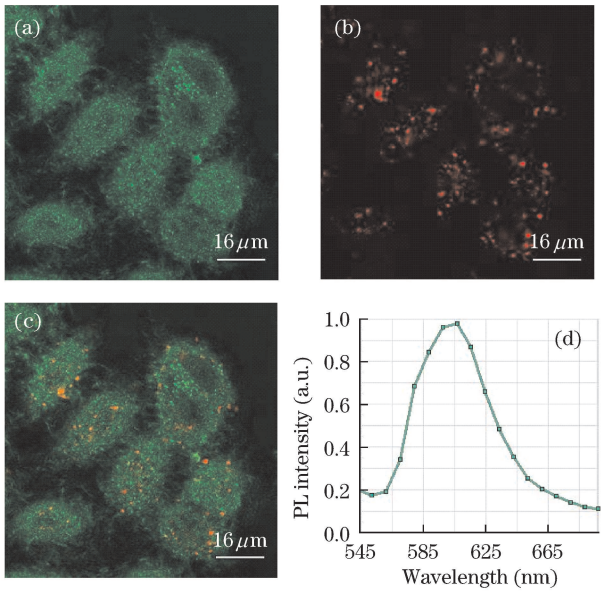

Fig. 3. Confocal reflection and fluorescence images of living HeLa cells stained by QDs-Tf bioconjugates. (a) Reflection image is pseudo-colored in green. The wavelength band for the reflection channel is 480−500 nm. (b) Fluorescence image is pseudo-colored in red. The wavelength band for the reflection channel is 580−620 nm. (c) Overlay image of reflection and fluorescence images. (d) Spectrum of the region-of-interest in (c).

Figure 4 shows the overview of the reconstructed 3D diagram of the cells at various rotations of angles. The 3D diagram of the cells suggested that the bioconjugated QDs were mostly accumulated around the nucleus after treated for 24 h, which was confirmed from fluorescence confocal sectioning images of these cells. In comparison with Fig. 3, the locations of bioconjugated QDs in the cells are clearer. Such 3D reconstruction evaluation provided evidences of inserted nanoparticles inside living cells.

In the present work, the fluorescence intensity of the bioconjugated QDs has been correlated with the uptake of bioconjugated QDs into HeLa cells. In general, in a single cell, the more bioconjugated QDs is labeled, the higher fluorescence intensity the cell shows. Based on this assumption, the sum of the gray level of each pixel of the reconstructed fluorescence signal could be taken as a quantificational parameter in describing the uptake quantity of bioconjugated QDs in the cells.

The uptake of QD bioconjugates in the living cells at different concentrations of bioconjugated QDs was investigated. The dosages were 1.0, 2.5, 5.0, 10.0, and 20.0 pmol, respectively. Figure 5 shows the relationship between dosage of QDs-Tf bioconjugates and their uptake by the living cells. The data indicate that no uptake is observed for a dosage as low as 1.0 pmol. Increasing the dosage from 2.5 to 10.0 pmol, the QDs fluorescence signal of the treated cells increases intensively. When the dosage is increased to above 10.0 pmol, the uptake reaches an equilibrium, which means the cells are saturated by QDs-Tf bioconjugates. We contribute this to the dynamic equilibrium process between Tf and the cells. Besides these positive control experiments, lysine-coated QDs formulation (unconjugated QDs) was used as a negative control group. Uptake of unconjugated QDs was less than that of conjugated QDs (results are not shown here). The internalization of the unconjugated QDs into the cells may be due to the nonspecific uptake

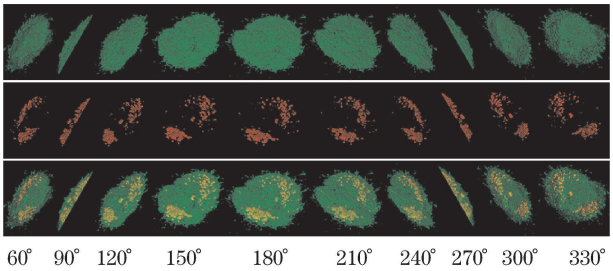

Fig. 4. 3D reconstructions of two living HeLa cells treated for 24 h (viewed from different angles). The upper panel shows confocal reflection images of the two cells, the middle panel shows confocal fluorescence images, and the bottom panel is for the overlay image of the upper and middle images.

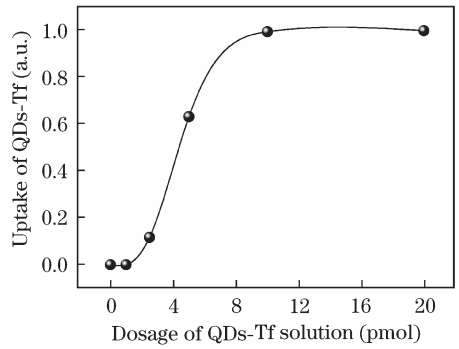

Fig. 5. Typical uptake of QDs-Tf bioconjugates by HeLa cells under different concentrations.

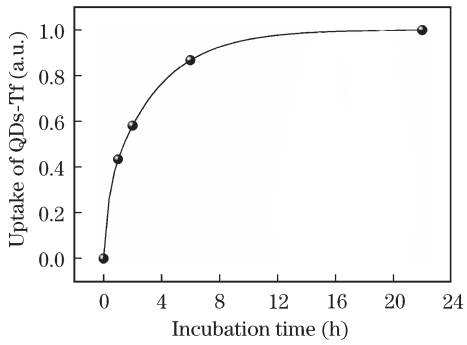

Fig. 6. Time dependence of uptake of QDs-Tf bioconjugates.

mechanism, which is commonly reported[17].

For the time-dependence studies, 5.0 pmol of QDs-Tf bioconjugates was used as an optimal dosage for HeLa cells labeling and imaging experiments. Figure 6 shows a plot of time-dependent uptake of bioconjugated QDs versus QD bioconjugates concentration. The uptake of QD bioconjugates in the cells increases with the incubation time, but with different internalization rates at different time points. The uptake of QD bioconjugates accomplishes from zero to almost 80% during the first 4 h of incubation. Then, the uptake slows down, and reaches a plateau stage.

In conclusion, both fluorescence confocal microscopy and 3D reconstruction techniques are used to quantitatively analyze the uptake and distribution of CdSe/CdS/ZnS QDs-Tf bioconjugates in living HeLa cells. The reconstructed 3D structure of cells indicates the precise localization of bioconjugates, and shows that the uptake of bioconjugated QDs in the cells is dosage and time dependent. The uptake of QDs by the HeLa cells increases with the increase of QDs-Tf concentration. However, when the QDs-Tf bioconjugates concentration exceeds 10 pmol, a plateau stage is reached and the uptake rate remains constant. In time-dependence studies, it is demonstrated that at a fixed dosage of 5 pmol, the uptake of QDs-Tf bioconjugates in the living cells increases gradually with the increase of incubation time. In addition, no morphological damage is observed in treated living cells. Both the MTS assay and confocal microscopic images demonstrate that such high luminescence bioconjugates have low cytotoxicity and could be used as efficient nanoprobes at non-cytotoxic dosages for ultrasensitive cancer sensing and targeted drug delivery. More importantly, by using 3D reconstruction technique, we are able to map the locations of the particles in living cells and study biodynamic process of the bioconjugates. This study may be an important fundamental work for future development of drug-QDs-Tf biodynamic nanoplatform applications.

This work was supported by the National Natural Science Foundation of China (Nos. 30900335, 60878053, and 60627003), the Guangdong Province Science Foundation (No. 2008078), the Natural Science Foundation of Shenzhen University, and the Start-Up Grant from Nanyang Technological University. Danni chen and Gaixia Xu contribute equally to this letter.

References

1. M. Bruchez, Jr., M. Moronne, P. Gin, S. Weiss, and A. P. Alivisatos, Science **281,** 2013 (1998).
2. W. C. W. Chan and S. Nie, Science **281,** 2016 (1998).
3. X. Michalet, F. F. Pinaud, L. A. Bentolila, J. M. Tsay, S. Doose, J. J. Li, G. Sundaresan, A. M. Wu, S. S. Gambhir, and S. Weiss, Science **307,** 538 (2005).
4. I. L. Medintz, H. T. Uyeda, E. R. Goldman, and H. Mattoussi, Nature Mater. **4,** 435 (2005).
5. L. Zhao, F. Wu, W. Tian, and C. Li, Acta Opt. Sin. (in Chinese) **29,** 1332 (2009).
6. L. Chen, Z. Guo, and X. Yang, Acta Opt. Sin. (in Chinese) **29,** 1320 (2009).
7. P. N. D. Slidke, R. Heintzmann, D. J. Arndt-Jovin, J. N. Post, H. E. Grecco, E. A. Jares-Erijman, and T. M. Jovin, Nature Biotechnol. **22,** 198 (2004).
8. A. M. Derfus, A. A. Chen, D. H. Min, E. Ruoslahti, and S. N. Bhatia, Bioconjugate Chem. **18,** 1391 (2007).
9. X. Gao and S. Nie, Trends in Biotechnol. **21,** 371 (2003).
10. J. Qian, K. T. Yong, I. Roy, T. Y. Ohulchanskyy, E. J. Bergey, H. H. Lee, K. M. Tramposch, S. He, A. Maitra, and P. N. Prasad, J. Phys. Chem. B **111,** 6969 (2007).
11. P. K. Sudeep, K. T. Early, K. D. McCarthy, M. Y. Odoi, M. D. Barnes, and T. Emrick, J. Am. Chem. Soc. **130,** 2384 (2008).
12. K. T. Yong, J. Qian, I. Roy, H. H. Lee, E. J. Bergey, K. M. Tramposch, S. He, M. T. Swihart, A. Maitra, and P. N. Prasad, Nano Lett. **7,** 761 (2007).
13. G. Xu, K.-T. Yong, I. Roy, S. D. Mahajan, H. Ding, S. A. Schwartz, and P. N. Prasad, Bioconjugate Chem. **19,** 1179 (2008).
14. D. F. Emerich and C. G. Thanos, J. Drug Targeting **15,** 163 (2007).
15. H. Sun, H. Li, and P. J. Sadler, Chem. Rev. **99,** 2817 (1999).
16. M. Manchester and P. Singh, Adv. Drug Delivery Rev. **58,** 1505 (2006).
17. K.-T. Yong, H. Ding, I. Roy, W.-C. Law, E. J. Bergey, A. Maitra, and P. N. Prasad, ACS Nano. **3,** 502 (2009).